Time-Resolved Fluorescence of Intestinal and Liver Fatty Acid Binding Proteins: Role of Fatty Acyl CoA and Fatty Acid†

Andrey Frolov and Friedhelm Schroeder*

Department of Physiology and Pharmacology, Texas A&M University, TVMC, College Station, Texas 77843-4466

Received June 11, 1996; Revised Manuscript Received November 13, 1996⊗

ABSTRACT: The effect of fatty acyl CoA and fatty acid on the solution structure and dynamics of two intestinal enterocyte fatty acid binding proteins, intestinal (I-FABP) and liver (L-FABP), was examined by time-resolved fluorescence of FABP aromatic amino acid residues. I-FABP Trp displayed two rotational correlation times, 6.6 and 0.4 ns, reflecting motion of the protein as a whole and segmental mobility of Trp. Neither oleoyl CoA, oleic acid, nor CoASH altered overall I-FABP rotational correlation time. However, oleic acid and CoASH increased I-FABP Trp segmental mobility, while oleoyl CoA and CoASH decreased I-FABP Trp limiting anisotropy (order). The angle of I-FABP Trp "wobbling in a cone" was increased by ligands in the order oleoyl CoA > CoASH > oleic acid. L-FABP Tyr also displayed two rotational correlation times, 6.6 and 0.05 ns, the latter being 8-fold faster than I-FABP Trp segmental mobility. L-FABP overall rotational motion, in contrast to that of I-FABP, was significantly increased by ligands in the order oleoyl CoA > oleic acid > CoASH. *cis*-Parinaric acid and *cis*-parinaroyl CoA bound to L-FABP also reflected overall L-FABP motion but yielded longer rotational correlation times, 8.2 and 10.7 ns, than the respective apo-FABPs. Such effects were not observed with I-FABP. Finally, both *cis*-parinaric acid and *cis*-parinaroyl CoA were much less ordered in the I-FABP ligand binding site than with L-FABP. These observations suggest that the rotational dynamics of L-FABP and its conformation are more sensitive to ligands than I-FABP. Further, ligands such as fatty acids, fatty acyl CoAs, and/or CoASH differentially modulate the I-FABP and L-FABP dynamics, and the ligand binding sites of these proteins differ in their ability to order the ligands.

To date at least seventeen intracellular lipid binding proteins have been identified [reviewed in Banaszak et al. (1994)]. At least ten belong to the fatty acid binding protein (FABP)[1] superfamily (Banaszak et al., 1994; Sacchettini & Gordon, 1993), of which five are expressed in intestine: intestinal fatty acid binding protein (I-FABP), liver fatty acid binding protein (L-FABP), cellular retinol binding protein-II (CRBP-II), gastrotropin, and ileal lipid binding protein (I-LBP) (Glatz & Veerkamp, 1985; Bass, 1988; Paulussen & Veerkamp, 1990; Kaikaus et al., 1990; Schroeder et al., 1993; Jakoby et al., 1993; Kanda et al., 1991; Miller & Cistola, 1993). However, only the L-FABP and I-FABP bind fatty acids with high affinity and are highly expressed (2−3% of cytosolic protein) in proximal ileal enterocytes where most fatty acid absorption/metabolism occurs. If both I-FABP and L-FABP fulfill the same function, the need for two fatty acid binding proteins coexisting at high concentrations (400−1000 μM) in proximal enterocytes is difficult to rationalize.

Some data suggest that subtle differences in the structures of these FABPs may give rise to differences in ligand binding specificities/properties (Banaszak et al., 1994; Schroeder et al., 1993). Despite apparent close tertiary conformation similarity, the structures of I-FABP and L-FABP differ in the orientation of the fatty acid in the holo-I-FABP. The fatty acid carboxyl group interacts ionically with an I-FABP Arg deep in the single binding site (reviewed in Sacchettini and Gordon (1993)]. In contrast, in holo-L-FABP the fatty acid carboxyl is suggested to be exposed at the protein surface in two fatty acid binding sites (Cistola et al., 1988, 1989). Furthermore, holo-I-FABP appears less thermostable and less pH-sensitive than holo-L-FABP (Banaszak et al., 1994; Ropson et al., 1990; Muga et al., 1993). Unfortunately, there is little information of ligand effects on conformational properties of these proteins in solution. Moreover and in contrast to I-FABP, X-ray crystal structures of apo- and holo-L-FABP are not available (Banaszak et al., 1994).

With rare exception (Jakoby et al., 1993), protein structural determinants for FABPs are not completely clear. Despite their three-dimensional structural similarity (Banaszak et al., 1994), I-FABP and L-FABP differ strikingly in ligand specificity. Other than one report (Jolly et al., submitted) no natural ligands except fatty acids have been shown to bind to I-FABP (Banaszak et al., 1994). In contrast, L-FABP binds fatty acids, fatty acyl CoAs, lysophospholipids, cholesterol, and other lipids (reviewed in Paulussen and Veerkamp (1990) and Schroeder et al., (1993)]. Although earlier results regarding L-FABP binding fatty acyl CoAs [reviewed in Paulussen and Veerkamp (1990)] were questioned (Rasmussen et al., 1990), it was recently shown that

* To whom correspondence should be addressed at Department of Physiology and Pharmacology, Texas A&M University, TVMC, College Station, TX 77843-4466. Phone: (409) 862-1433. FAX: (409) 862-4929. E-mail: fschroeder@cvm.tamu.edu.

† This work was supported in part by a grant from the United States Public Health Service, NIH (DK41402).

⊗ Abstract published in *Advance ACS Abstracts,* January 1, 1997.

[1] Abbreviations: FABP, fatty acid binding protein; I-FABP, intestinal fatty acid binding protein; L-FABP, liver fatty acid binding protein; CoASH, coenzyme A; *cis*-parinaric acid, 9*Z*,11*E*,13*E*,15*Z*-octadecatetraenoic acid; *cis*-parinaroyl CoA, 9*Z*,11*E*,13*E*,15*Z*-octadecatetraenoyl coenzyme A; dimethyl POPOP, (1,4-bis[4-methyl-5-phenyl-2-oxazolyl]-benzene).

S0006-2960(96)01392-X CCC: $14.00

L-FABP clearly binds fatty acyl CoAs with 2:1 stoichiometry (Hubbell et al., 1994; Rolf et al., 1995).

Finally, limited evidence indicates that both of these proteins function other than in simply binding fatty acid molecules. A variety of studies with isolated enzymes or membrane fractions *in vitro* indicate that L-FABP may function in fatty acid transfer and stimulate formation of lipidic macromolecules from fatty acids (reviewed in Paulussen and Veerkamp (1990), Schroeder et al. (1993), and Hubbell et al. (1994)]. Similar studies with I-FABP have not been reported or were negative (Hubbell et al., 1994; Jefferson et al., 1991). Nevertheless, differential effects of L-FABP vs I-FABP expression in intact transfected L-cells indicate that I-FABP, but not L-FABP, stimulates preferential incorporation of exogenously added radiolabeled oleic acid into intracellular triglycerides and cholesteryl esters 5.6- and 1.4-fold, respectively (Prows et al., 1995, 1996). Furthermore, a recent report showed that the affinity of I-FABP for fatty acid correlates with fatty acid oxidation and insulin resistance in humans (Baier et al., 1995). These observations also suggest that I-FABP may have a role in fatty acyl CoA metabolism.

The objectives of the present investigation were to (i) examine the L-FABP and I-FABP structure in solution by using time-resolved fluorescence spectroscopy; (ii) determine the effects of fatty acyl CoAs on the hydrodynamic properties of L-FABP and I-FABP; and (iii) characterize the structural order and dynamics of fatty acyl CoAs inside the L-FABP and I-FABP binding pockets.

MATERIALS AND METHODS

Materials. *cis*-Parinaric acid was from Molecular Probes (Eugene, OR). *cis*-Parinaroyl CoA was synthesized (Hubbell et al., 1994). Oleoyl-coenzyme A, oleic acid, coenzyme A (CoASH), palmitic acid, hexadecanedioic acid, acyl-coenzyme A synthase for preparation of *cis*-parinaroyl CoA, adenosine 5′-triphosphate (ATP), 1,4-bis[4-methyl-5-phenyl-2-oxazollyl]benzene (dimethyl POPOP), *p*-terphenyl, and (hydroxymethyl)aminomethane (Tris) were obtained from Sigma Chemical Co. (St. Louis, MO). All other chemical were reagent grade or better.

Methods. Recombinant L-FABP from the *E. coli* strain carrying plasmid pJBL2 for L-FABP and recombinant I-FABP from the *E. coli* strain carrying plasmid pIFABPexp6 for I-FABP were purified as described earlier (Lowe et al., 1984, 1987). The purified FABPs were delipidated as described previously (Glatz & Veerkamp, 1983; Nemecz et al., 1991a,b) unless otherwise specified. The protein concentration was determined (Bradford, 1976) and corrected according to amino acid analysis (Lowe et al., 1984). The Bradford protein assay overestimates the concentration of L-FABP 1.69-fold and I-FABP 1.07-fold.

Absorption and Steady-State Fluorescence Spectroscopy. Absorption spectra were measured at room temperature (~23 °C) using a UV/vis Lambda 2 double-beam spectrophotometer (Perkin-Elmer Inc., Norwalk, CT). Corrected (unless otherwise noted) steady-state fluorescence spectra were measured in 1 cm path length quartz fluorescence cuvettes with a PC1 photon-counting spectrofluorimeter (ISS Inc., Champaign, IL). Sample temperature in the cuvette was maintained at 25 °C (±0.1 °C) with a thermostated cell holder. The excitation and emission bandwidths were 4 and 8 nm, respectively.

Binding of nonfluorescent fatty acyl CoAs with a 2:1 stoichiometry to L-FABP has been reported by several laboratories (Hubbell et al., 1994; Rolf et al., 1995; Paulussen & Veerkamp, 1990). The specific nature and completeness of *cis*- and *trans*-parinaric acid as well as *cis*- and *trans*-parinaroyl CoA were ascertained by the following criteria: (i) The specific binding of *cis*(*trans*)-parinaric acid to L-FABP and I-FABP (Nemecz et al., 1991a) as well as the specific binding of *cis*-parinaroyl CoA binding to L-FABP (Hubbell et al., 1994) were reported earlier by our group. Unfortunately, due to high noise levels under the assay conditions used to measure *cis*-parinaroyl CoA binding to I-FABP, reliable data on the binding of *cis*-parinaroyl CoA to I-FABP were not obtained (Hubbell et al., 1994). Those technical problems have been successfully resolved, and recently I-FABP was shown to bind fatty acyl CoAs specifically and with a high affinity (Gossett et al., 1996; Jolly et al., submitted). Furthermore, L-FABP bound up to two fatty acids or two fatty acyl CoA binding sites while I-FABP bound one fatty acid or one fatty acyl CoA (Nemecz et al., 1991a; Hubbell et al., 1994; Gossett et al., 1996; Jolly et al., submitted). Nonspecific binding sites were not observed (Nemecz et al., 1991a; Hubbell et al., 1994; Jolly et al., submitted). (ii) In the present study, the initial experimental conditions were chosen based on the known binding characteristics of *cis*(*trans)*-parinaric acids (Nemecz et al., 1991a) and *cis*(*trans*)-parinaroyl CoAs (Hubbell et al., 1994; Jolly et al., submitted) for L-FABP and I-FABP in order to reach maximal saturation of the protein with ligand (when protein fluorescence characteristics were measured) or to minimize unbound ligand [when *cis*(*trans*)-parinaric acid and *cis*(*trans*)-parinaroyl CoA fluorescence parameters were under investigation]. The experimental conditions were further optimized by titration of a fixed concentration of the protein with increasing amounts of a ligand or vice versa while observing the fluorescence intensity, fluorescence lifetimes, and fluorescence anisotropy reaching a saturation level. Because protein and ligand excitation and emission characteristics differed sufficiently, correction for the unbound ligand was found to be unnecessary. (iii) All fatty acids were used in the form of sodium salts in order to increase their aqueous solubility and to avoid the appearance of possible artifacts due to fatty acid solubility and/or protein interaction with fatty acid micelles. The fatty acid salts have much higher solubility in aqueous as compared to the free acids, as shown by almost a 1000-fold difference in the respective values of the critical micellar concentration, several millimoles vs several micromoles (Pryde, 1979; Small, 1986). Since the maximal fatty acid concentration in the present study never exceeded 10 μM (far below the 2 mM critical micellar concentration for typical C18 fatty acid sodium salts) (Small, 1986), the formation of the *cis*(*trans*)-parinaric acid micelles resulting in altered fatty acid binding and/or distortion of the protein structure was highly unlikely.

Time-Resolved Fluorescence Spectroscopy. Time-resolved fluorescence measurements were performed with a GREG 250 subnanosecond multifrequency cross-correlation and modulation fluorimeter with KOALA sample compartment (ISS Inc., Champaign, IL). The excitation path contained a Glan−Taylor polarizer. The light source was an Innova-Sabre argon ion laser (Coherent Laser Group, Palo Alto, CA). This laser featured automatic wavelength selection in a multiline UV mode with the single lines at $\lambda = 275.4$, 300.2, 302.4, and 305.5 nm and continuous power output of 340,

630, 800, and 460 mW, respectively. The laser output was kept stable over several hours in either the "Power Track" or the "Light Regulation" mode. In order to avoid appearance of artifacts due to scattered emission and Raman scatter, the protein fluorescence was observed from samples placed in a quartz fluorescence cuvette, optical path length 0.3 cm (Expotech Inc., Houston, TX). Protein aromatic amino acid fluorescence emission was selected with 313 BP10 (for detection of Tyr) and the 341 BP15 (for detection of Trp) interference filters (Omega Optical Inc., Brattleboro, VT) having transmittance maxima at $\lambda = 313$ nm (bandwidth 10 nm) and $\lambda = 341$ nm (bandwidth 15 nm), respectively. Excitation intensity was optimized to minimize protein photobleaching (typically $\leq$ 10%) and to maximize signal to noise ratio. *cis*-Parinaric acid and *cis*-parinaroyl CoA were excited at $\lambda = 325$ nm by a 4240NB He-Cd laser (Liconix, Sunnyvale, CA), and emission was observed through a KV389 low-fluorescent cutoff filter (Schott Glass Technologies Inc., Duryea, PA). To avoid inner filter artifacts, sample absorbance at the excitation wavelengths was $\leq$0.05. All data were obtained in 25 mM phosphate buffer, pH 7.4 at 25 °C.

Fluorescence Lifetime Data Acquisition and Analysis. Fluorescence decay kinetics were measured with the excitation polarizer oriented at 35° to yield rotation-free results (Spencer & Weber, 1970). Fluorescence lifetime data were acquired and analyzed at 12−15 modulation frequencies (20−225 MHz). External lifetime standards for measurement of protein Tyr, protein Trp, *cis*-parinaric acid, and *cis*-parinaroyl CoA fluorescence decay were *p*-terphenyl in absolute ethanol ($\tau = 1.05$ ns) and dimethyl POPOP in absolute ethanol ($\tau = 1.45$ ns), respectively. Data were acquired until the limit of standard error was reached: 0.20° and 0.004, for phase and modulation, respectively. ISS-187 Software (ISS Inc., Champaign, IL) was employed for data collection and analysis. Fluorescence was analyzed as a sum of exponentials: $I(t) = \sum\alpha_i \exp(-t/\tau_i)$, where τ_i is lifetime and α_i is a preexponential factor, $\sum\alpha_i = 1$. Fractional intensity, f_i, was expressed as $f_i = \alpha_i\tau_i/\sum\alpha_i\tau_i$. The minimized χ^2 parameter was used as a criterion for best fit to the applied model. Generally, a χ^2 value less than 3 was considered to be acceptable (Parasassi et al., 1984).

Anisotropy Decay Measurement and Analysis. Time-resolved anisotropy data were obtained at 12−15 modulation frequencies for both $I_{\|}$ and $I_{\perp}$ component over the range of 20−225 MHZ with Glan−Taylor and Glan−Thompson polarizers in the excitation and emission channels, respectively. Standard error limits were set to 0.02°, 0.004, and 0.01 for the measurement of phase, modulation, and polarization, respectively. The fluorescence anisotropy decay was modeled by a sum of exponentials as $r(t) = r(0)\Sigma g_i \exp(-t/\theta_i)$, where $r(0)$ is the anisotropy of a fluorophore at time 0, θ_i, is the rotational correlation time, and g_i is fractional anisotropy. Best fits were obtained as described above using ISS-187 Software (ISS Inc., Champaign, IL).

cis-Parinaric Acid Displacement Assay. L-FABP (0.1 μM) or I-FABP (0.1 μM) in phosphate-buffered saline (pH 7.4) was incubated with *cis*-parinaric acid (0.3 μM) for 5 min at room temperature until maximal fluorescence was achieved. L-FABP- or I-FABP-bound *cis*-parinaric acid was displaced by increasing palmitic acid or thapsic acid. All measurements were corrected for the appropriate blank (ligand only and protein only) and for photobleaching.

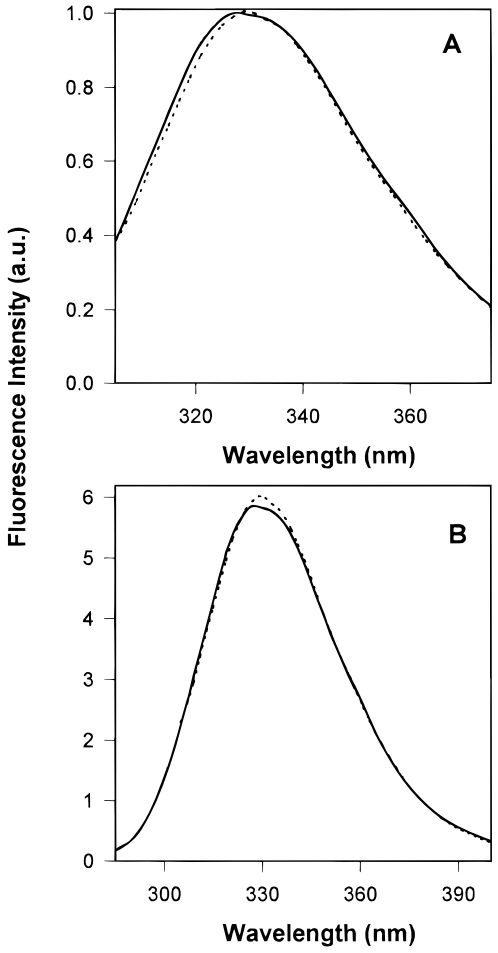

FIGURE 1: Fluorescence emission spectra of apo-I-FABP. Spectra were obtained at 25 °C as in Methods. (A) 1.15 μM I-FABP in PBS, pH 7.4, upon excitation at 270 (solid line) and 296 nm (dotted line). (B) I-FABP fluorescence emission spectra obtained for excitation at 270 (solid line) and 296 nm (dotted line) were normalized at 380 nm, where only Trp emits.

RESULTS

I-FABP Aromatic Amino Acid Fluorescence Properties

Apo-I-FABP Steady-State Fluorescence. I-FABP contains four Tyr and two Trp residues (Gordon J. I., & Lowe, 1985; Sweetser et al., 1987a,b), which may contribute to the observed protein emission. Since emission maxima of Tyr and Trp in proteins are near 304 and 340 nm, respectively, the relative contributions of these amino acids to I-FABP fluorescence emission were resolved by varying the excitation wavelength to selectively excite Trp at 296 nm or both Tyr and Trp simultaneously at 270 nm. If the I-FABP fluorescence spectrum were to be significantly blue shifted and broadened in bandwidth (full width at half-height) upon excitation at 270 nm, as compared to that of 296 nm, this would signify increased contribution of direct Tyr emission to the total I-FABP fluorescence.

Excitation of I-FABP at 270 nm (Figure 1A, solid line), 280 nm (not shown), and 296 nm (Figure 1A, dotted line) did not result in significant alterations in fluorescence emission maxima (328, 330, and 331 nm, respectively) or bandwidth (50, 48, and 47, respectively). When I-FABP was excited at 296 nm and emission spectra were normalized to the intensity at 380 nm (where tyrosine emission can not be seen), both fluorescence emission spectra were undistinguishable in the region of 290−315 nm where the maximum

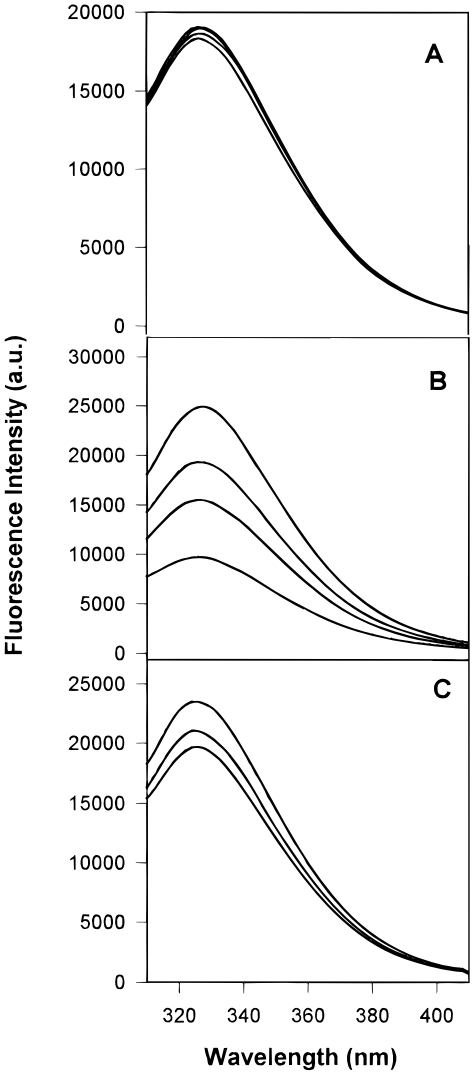

FIGURE 2: Ligand effect on fluorescence emission of I-FABP. (A) Uncorrected fluorescence spectra of I-FABP (1.15 μM) in PBS, pH 7.4, upon excitation at 280 nm. From top to bottom: I-FABP only; I-FABP + 1 μM oleic acid; I-FABP + 2 μM oleic acid, and I-FABP + 5 μM oleic acid. (B) I-FABP only; I-FABP + 2 μM oleoyl CoA; I-FABP + 4 μM oleoyl CoA, and I-FABP + 8 μM oleoyl CoA. (C) I-FABP only; I-FABP + 0.4 μM coenzyme A; I-FABP + 1.2 μM coenzyme A, and I-FABP + 4.1 μM coenzyme A.

of Tyr emission might have been expected (Figure 1B). This observation is consistent with the absence of a Tyr emission component in I-FABP fluorescence. The lack of Tyr emission in I-FABP does not, however, rule out the possibility of indirect Tyr involvement in the protein fluorescence via the radiationless energy transfer to I-FABP Trp residues. In summary, it appears that fluorescence of apo-I-FABP is predominantly due to emission of protein Trp(s). Furthermore, both the position of I-FABP emission peak (~330 nm) and its bandwidth (~50 nm) are consistent with the Trp(s) being located in rather hydrophobic protein loci (Burstein et al., 1973).

Holo-I-FABP Steady-State. The effect of ligands on I-FABP Trp emission spectra was determined. Addition of up to 5 molar equiv of oleic acid to I-FABP excited at 296 nm did not significantly alter I-FABP Trp emission intensity or the shape of its Trp emission spectrum (Figure 2A). In contrast, titration of I-FABP with increasing amount of oleoyl CoA dramatically reduced I-FABP Trp emission by almost 63% when the I-FABP:ligand molar ratio was 1:8 (Figure 2B). The position of the I-FABP fluorescence emission peak was not affected by oleoyl CoA (Figure 2B). Coenzyme A by itself also quenched fluorescence of I-FABP Trp but with less efficiency than observed with oleoyl CoA, reducing I-FABP Trp emission 17% at 4 molar equiv of CoASH added (Figure 2C). Again, the shape of I-FABP Trp fluorescence emission spectrum remained unchanged. It should be noted that no detectable fluorescence quenching was observed when an equivalent amount of free tryptophan (as compared to I-FABP concentration) was titrated with the same ligands over the concentration ranges used above (data not shown). In summary, oleoyl CoA and coenzyme A, but not oleic acid, quenched I-FABP Trp emission.

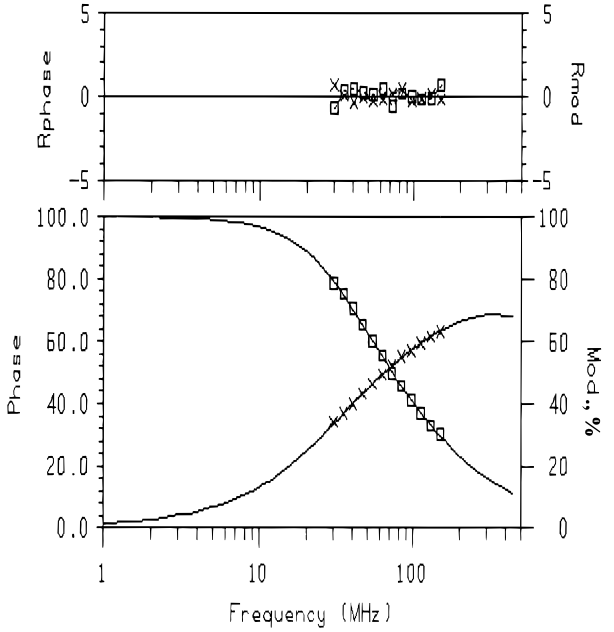

FIGURE 3: Frequency response of I-FABP fluorescence decay. I-FABP (2 μM) was in PBS at 25 °C. Excitation and emission wavelengths were 300 and 341 nm, respectively. The data best fit a two-component analysis with χ^2 of 1.9.

Apo-I-FABP Fluorescence Lifetime. Although the lack of I-FABP Trp emission shift in I-FABP interacting with ligands (oleoyl CoA and fatty acid) was consistent with the I-FABP Trp localized in a hydrophobic environment, the emission maximum at 330 nm could also reflect contributions of ordered water in the binding site (Sacchettini & Gordon, 1993). Thus, the polarity of the ligand binding site can still be influenced by ordered water even though this cannot be detected by steady-state emission maxima. Apo-I-FABP Trp fluorescence emission decay was biexponential (Figure 3), with the presence of major and minor components (Table 1) typical for proteins with multiple Trp residues (Lakowicz et al., 1983; Demchenko, 1986). When I-FABP was excited at 275 nm and emission was detected at 341 nm, the lifetimes of the major and minor components were 4.41 ns (fraction 0.69) and 1.91 ns (fraction 0.31), respectively (Table 1). When I-FABP was excited at 275 nm and emission was detected at 313 nm, no differences in lifetime components were detected except that the fraction of the short-lifetime component tended to increase from 0.31 to 0.42 (Table 1). In contrast, upon exciting I-FABP Trp at 300 nm and measuring Trp emission at 341 nm, lifetimes were unaffected but the fraction f_2 representing component 2 was significantly reduced to 0.25 (Table 1). As a result, when Trp was excited at λ_{exc} = 275 nm and emission was detected at λ_{exc} = 313 nm, the mean lifetime, 3.29 ns, was significantly lower than

Table 1: Fluorescence Decay of I-FABP[a]

ex/emiss.	τ_1 (ns)	τ_2 (ns)	f_1	f_2	$\tilde{\tau}$[b] (ns)
275/313	4.47 ± 0.10	1.70 ± 0.01	0.58 ± 0.02	0.42 ± 0.02	3.29 ± 0.03
275/341	4.41 ± 0.06	1.91 ± 0.08	0.69 ± 0.04	0.31 ± 0.04	3.66 ± 0.04[c]
300/341	4.66 ± 0.04	1.78 ± 0.02	0.75 ± 0.03[c]	0.25 ± 0.03[c]	3.93 ± 0.02[c]

[a] The fluorescence of I-FABP (2 μM) was analyzed by a sum of exponentials as $I(t) = \sum\alpha_i \exp(-t/\tau)$ where $\sum\alpha_i = 1$ and $f_i = \alpha_i\tau_i/\sum\alpha_i\tau_i$. The fraction of the light scatter for all samples was ≤0.03. All measurements were made in PBS (pH 7.4) at 25 °C. Values represent the mean ±SE ($n = 5-6$). [b] Mean fluorescence lifetime $\tilde{\tau}$ was calculated as $\tilde{\tau} = \sum f_i\tau_i$. [c] $p < 0.05$ as compared to 275/313 excitation/emission.

Table 2: Ligand Effect on Fluorescence Decay of I-FABP[a]

ligand	τ_1 (ns)	τ_2 (ns)	f_1	f_2	$\tilde{\tau}$[b] (ns)
none	4.66 ± 0.04	1.78 ± 0.02	0.75 ± 0.03	0.25 ± 0.03	3.93 ± 0.03
oleic acid	4.32 ± 0.04[c]	1.54 ± 0.05[c]	0.84 ± 0.01	0.16 ± 0.01	3.87 ± 0.01
oleoyl CoA	3.95 ± 0.08[c]	0.62 ± 0.02[c]	0.85 ± 0.01[c]	0.15 ± 0.01[c]	3.46 ± 0.07[c]
CoASH	4.79 ± 0.10	2.04 ± 0.01	0.74 ± 0.02	0.26 ± 0.02	4.07 ± 0.30

[a] All conditions and details were as described in the legend to Table 1. The ligand concentration was 5-fold molar excess over I-FABP. Excitation and emission wavelengths were 300 nm and 341 nm, respectively. [b] Mean fluorescence lifetime $\tilde{\tau}$ was calculated as $\tilde{\tau} = \sum f_i\tau_i$. [c] $p < 0.05$ as compared to no ligand ($n = 5-6$).

the lifetime of I-FABP Trp, 3.93 ns, when Trp was excited and detected ($\lambda_{exc} = 300$ nm; $\lambda_{exc} = 341$ nm)(Table 1). Therefore, the increased lifetime of I-FABP Trp when detected at the red edge of excitation was consistent with solvent relaxation around the excited Trp residue in I-FABP.

Holo-I-FABP Fluorescence Lifetime. The effect of ligand binding (holo-I-FABP) on Trp fluorescence emission decay kinetics of apo-I-FABP is summarized in Table 2. Addition of 5 molar equiv of oleic acid to apo-I-FABP caused a small but significant reduction of both Trp lifetime components, from 4.66 to 4.32 ns and from 1.78 to 1.54 ns, respectively. No visible alterations of their respective fractions were detected. However, the modest changes in I-FABP Trp emission lifetime upon interaction with oleic acid were insufficient to significantly alter the mean lifetime of I-FABP Trp (Table 2). In contrast to these observations with a free fatty acid, addition of a fatty acyl CoA significantly altered both lifetimes and fractions of I-FABP Trp. Oleoyl CoA caused a more prominent effect on fluorescence lifetime of I-FABP, decreasing the long component from 4.66 to 3.95 ns and the short component from 1.78 to 0.62 ns. Oleoyl CoA also decreased the fraction of the short-lifetime component by 40% from 0.25 to 0.15 (Table 2). These alterations of I-FABP Trp lifetimes and fractions induced by oleoyl CoA were reflected as a significant reduction in mean lifetime from 3.93 to 3.46 ns (Table 2). Under the same conditions CoASH did not detectably affect I-FABP Trp emission lifetimes or fractions (Table 2).

Apo-I-FABP Time-Resolved Anisotropy. Time-resolved fluorescence anisotropy provides information on the rotational motions in I-FABP on nanosecond and subnanosecond time scales. The anisotropy decay of apo-I-FABP Trp displayed two correlation times, 6.57 and 0.40 ns (Figure 4; Table 3). The rapid component is attributed to the segmental motion of Trp, while the longer component reflects the rotational diffusion of the entire protein globule (Lakowicz et al., 1987; Elofsson et al., 1991). In the case of proteins such as I-FABP with several Trp residues the measured short correlation time represents an average residue mobility in excess of the overall protein rotational diffusion (Lakowicz et al., 1987). The measured I-FABP rotational correlation time of 6.57 ns is consistent with that expected for a protein of that size, 15 kDa (Cantor & Schimmel, 1980). The measured short rotational component indicates that Trp

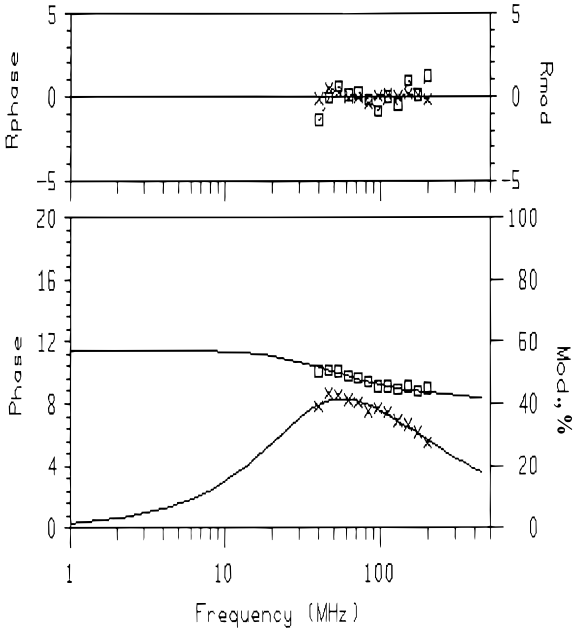

FIGURE 4: Frequency response of I-FABP anisotropy decay. I-FABP (2 μM) was in PBS at 25 °C. Excitation and emission wavelengths were 300 and 341 nm, respectively. The data best fit a two-component analysis with χ^2 of 2.0.

undergoes fast rotational motions in apo-I-FABP. The amplitude of Trp torsional motions can be obtained by employing eq 1 (Lipari & Szabo, 1980):

$$r/r(0) = (3\cos^2\phi - 1)/2 \quad (1)$$

where, $r(0)$ is the maximal anisotropy at time 0, and $r(0) = r(0)g_1 + r(0)g_2$ (Table 3); r is the remaining anisotropy (the anisotropy after the segmental rotation of Trp is completed) and is defined as $r = r(0)g_1$ (Table 3); ϕ is the angle through which Trp is able to rotate. The calculated ϕ value for apo-I-FABP was 11° (Table 3), which is consistent with the existence of some spacial restrictions imposed by the protein matrix on the rotation of Trp in apo-I-FABP.

Holo-I-FABP Time-Resolved Anisotropy. The effects of ligands on I-FABP Trp time resolved anisotropy decay are presented in Table 3. Ligand binding could affect the rates of motion of the entire I-FABP protein, the segmental motion of I-FABP Trp, and the restriction to motion (limiting

Table 3: Ligand Effect on Anisotropy Decay of I-FABP[a]

ligand	θ_1 (ns)[b]	θ_2 (ns)	$r(0)g_1$[c]	$r(0)g_2$	"wobbling" cone angle (deg)[d]
none	6.57 ± 0.22	0.40 ± 0.01	0.313 ± 0.005	0.020 ± 0.003	11
oleic acid	6.21 ± 0.08	0.50 ± 0.03[e]	0.312 ± 0.002	0.040 ± 0.001[e]	16
oleoyl CoA	6.51 ± 0.01	0.47 ± 0.07	0.226 ± 0.010[e]	0.105 ± 0.010[e]	27
CoASH	6.73 ± 0.30	0.73 ± 0.03[e]	0.282 ± 0.020[e]	0.050 ± 0.020[e]	18

[a] The anisotropy of tryptophan in I-FABP (2 μM) with or without 5-fold molar excess of ligand was analyzed by a sum of exponentials as $r(t) = r(0)\sum g_i \exp(-t/\theta_i)$. [b] $\lambda_{exc} = 300$ nm; $\lambda_{em} = 341$ nm. [c] $r(0)$ was allowed to vary. [d] The "wobbling" cone angle was calculated for the I-FABP tryptophan on the basis of time-resolved fluorescence anisotropy data presented in the Table and by using the following equation: $r/r(0) = (3\cos^2\phi - 1)/2$, where r is the residual (limiting) anisotropy, and $r(0)$ is the sum of $r(0)g_1 + r(0)g_2$. The sum of $g_1 + g_2 = 1$. [e] $p < 0.05$ as compared to no ligand ($n = 5-6$).

Table 4: Ligand Effect on Fluorescence Decay of L-FABP[a]

ligand	τ_1 (ns)	τ_2 (ns)	f_1	f_2	$\tilde{\tau}$[b] (ns)
none	3.56 ± 0.10	1.30 ± 0.003	0.54 ± 0.01	0.46 ± 0.01	2.53 ± 0.02
oleic acid	3.17 ± 0.20[c]	1.40 ± 0.004[c]	0.59 ± 0.04	0.41 ± 0.04	2.43 ± 0.05
oleoyl CoA	2.30 ± 0.06[c]	0.81 ± 0.003[c]	0.62 ± 0.03[c]	0.38 ± 0.03[c]	1.73 ± 0.003[c]
CoASH	3.69 ± 0.22	1.62 ± 0.06	0.41 ± 0.05	0.59 ± 0.05	2.46 ± 0.02

[a] The fluorescence of L-FABP (2 μM) with or without 5-fold molar excess of ligand was analyzed by a sum of exponentials as $I(t) = \sum\alpha_i \exp(-t/\tau_i)$ where $\sum\alpha_i = 1$ and $f_i = \alpha_i\tau_i/\sum\alpha_i\tau_i$. The fraction of the light scatter for all samples was ≤ 0.02. All measurements were made in PBS (pH 7.4) at 25 °C. The excitation and emission wavelengths were 275 and 313 nm, respectively. Values represent the mean ± SE ($n = 5-6$). [b] Mean fluorescence lifetime $\tilde{\tau}$ was calculated as $\tilde{\tau} = \sum f_i\tau_i$. [c] $p < 0.05$ as compared to no ligand ($n = 5-6$).

anisotropy or order or wobbling cone angle) of Trp in I-FABP. Different effects were observed depending upon the ligand interacting with I-FABP. Addition of 5 molar equiv of oleic acid to the I-FABP did not affect the overall protein rotation, θ_1, but affected intrinsic motions of Trp in I-FABP. Oleic acid increased I-FABP Trp segmental mobility, θ_2, from 0.4 to 0.5 ns, as well as the Trp maximal anisotropy, $r(0)$, from 0.333 to 0.352. The overall effect was measured as an increased I-FABP Trp wobbling cone angle, ϕ, from 11 to 16° (Table 3). Thus, oleic acid modestly increased I-FABP Trp rotational freedom. Under the same conditions oleoyl CoA altered I-FABP segmental mobility differently from oleic acid (Table 3). While oleoyl CoA was without effect on either the overall I-FABP or the I-FABP Trp segmental rotational correlation time, it dramatically altered the limiting anisotropy (order) portion of I-FABP Trp segmental mobility. Oleoyl CoA decreased I-FABP Trp limiting anisotropy (r_0g_1) from 0.313 to 0.226 (Table 3). The overall effect of oleoyl CoA was a 2.5-fold increase in the wobbling cone angle ϕ value, from 11 to 27°, demonstrating an oleoyl CoA-induced increase of I-FABP Trp rotational freedom. However, the rate of rotation did not change, thereby illustrating that this kinetic parameter (rate of rotation) is independent of the order parameters (maximal anisotropy, wobbling cone angle, etc.). CoASH by itself exhibited a third pattern of ligand effect on I-FABP and I-FABP Trp rotational dynamics. Like oleic acid and oleoyl CoA, CoASH did not alter the overall rotational dynamics of the I-FABP (Table 3). Unlike either oleic acid or oleoyl CoA, CoASH increased the Trp segmental mobility (correlation time θ_2) 1.8-fold from 0.4 to 0.73 ns. As with oleoyl CoA, CoASH significantly decreased I-FABP Trp limiting anisotropy (r_0g_1), from 0.313 to 0.282. The overall effect of CoASH on I-FABP was to increase the wobbling cone angle, ϕ, from 11 to 18° (Table 3). In general, rotational dynamics of I-FABP Trp, but not overall motion of the I-FABP protein as a whole, appeared very sensitive to the interaction of this protein and ligands, such as oleic acid, oleoyl CoA, and CoASH. Even though the specific effects on the segmental dynamics of these ligands differed, I-FABP binding of all three ligands increased the I-FABP Trp wobbling cone angle in the order oleoyl CoA > CoASH > oleic acid.

L-FABP Aromatic Amino Acid Fluorescence Properties

Apo- and Holo-L-FABP Steady-State Fluorescence Emission. L-FABP has three Tyr and no Trp residues (Gordon & Lowe, 1985; Sweetser et al., 1987a). Upon excitation at 275 nm the corrected fluorescence spectrum of apo-L-FABP displayed a single maximum at 303 nm, bandwidth of 65 nm (Figure 5A). Titration of L-FABP with up to 5-fold molar excess oleic acid quenched L-FABP Tyr emission intensity by less than 10% (Figure 5B). In contrast, 5-fold molar excess oleoyl acyl CoA quenched L-FABP Tyr fluorescence emission by 35% (Figure 5C). CoASH did not significantly affect L-FABP Tyr emission (Figure 5D). It should be noted that no detectable fluorescence quenching was observed when an equivalent amount of free Tyr in solution (as compared to L-FABP concentration) was titrated with the same ligands over same concentration range (data not shown).

Apo- and Holo-L-FABP Fluorescence Lifetime. The fluorescence decay of apo-L-FABP exhibited biexponential decay [$\tau_1 = 3.56$ ns (fraction 0.54); $\tau_2 = 1.3$ ns (fraction 0.46)] resulting in a mean lifetime of 2.53 ns (Table 4). Addition of 5 molar equiv of oleic acid decreased the L-FABP Tyr long-lifetime component from 3.56 to 3.17 while concomitantly slightly increasing the short-lifetime component from 1.3 to 1.4 ns. Consequently, the mean lifetime of L-FABP Tyr was unaltered by oleic acid. In contrast, oleoyl CoA had much larger effects on L-FABP Tyr lifetime values than did oleic acid. Oleoyl CoA decreased the two L-FABP Tyr lifetime components from 3.56 to 2.3 ns and from 1.3 to 0.81 ns, respectively (Table 4). Furthermore, this decrease of L-FABP Tyr fluorescence lifetimes was accompanied by a significant redistribution of their fractions, with the fraction of the long component being increased from 0.54 to 0.62. As a result, oleoyl CoA binding decreased the mean lifetime of L-FABP Tyr from 2.53 to 1.73 ns (Table 4). CoASH alone did not affect the L-FABP fluorescence decay kinetics (Table 4).

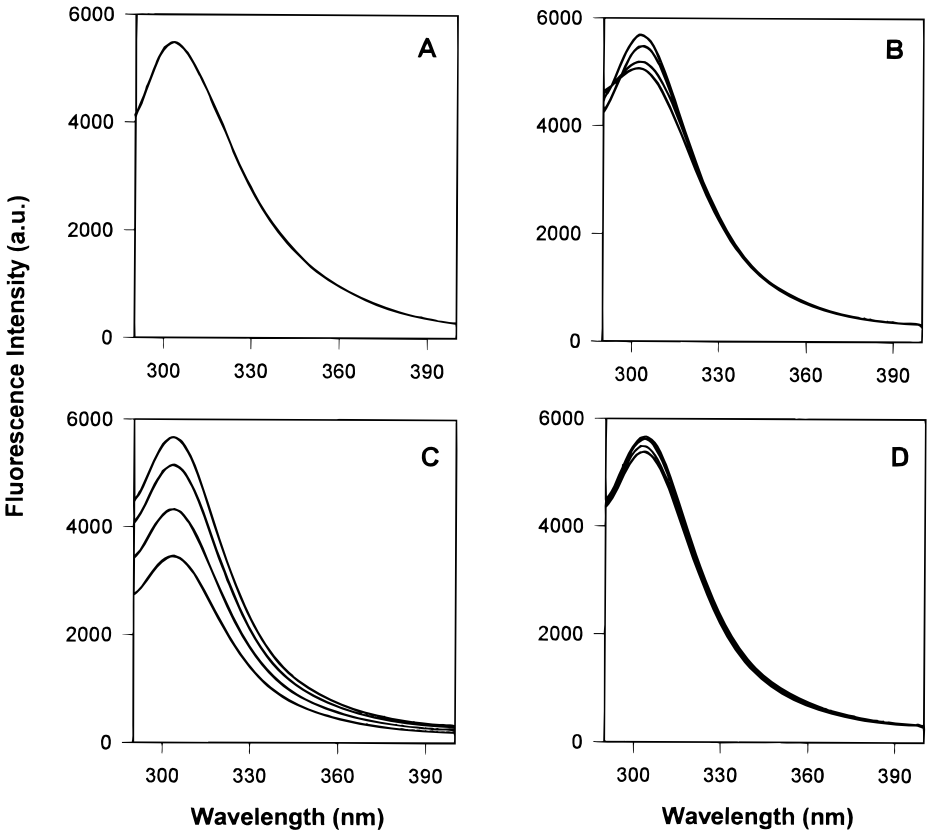

FIGURE 5: Fluorescence emission spectra apo- and holo-L-FABP. (A) Fluorescence spectra of apo-L-FABP (1.15 μM) in PBS, pH 7.4, with excitation at 275 nm. (B) Uncorrected fluorescence emission spectra of L-FABP in the presence of oleic acid. From top to bottom: L-FABP only; L-FABP + 1 μM oleic acid; L-FABP + 2 μM oleic acid, and L-FABP + 5 μM oleic acid. (C) Uncorrected fluorescence emission spectra of L-FABP in the presence of oleoyl CoA. From top to bottom: L-FABP only; L-FABP + 2 μM oleoyl CoA; L-FABP + 4 μM oleoyl CoA, and L-FABP + 8 μM oleoyl CoA. (D) Uncorrected fluorescence emission spectra of L-FABP in the presence of coenzyme A. From top to bottom: L-FABP only; L-FABP + 0.4 μM coenzyme A; L-FABP + 1.2 μM coenzyme A, and L-FABP + 4.1 μM coenzyme A.

Table 5: Ligand Effect on Anisotropy Decay of L-FABP[a]

ligand	θ_1 (ns)[b]	θ_2 (ns)	$r(0)g_1$	$r(0)g_2$	"wobbling" cone angle (deg)[e]
none	6.59 ± 0.10	0.05 ± 0.01	0.232 ± 0.002[c]	0.088 ± 0.002	25
oleic acid	5.24 ± 0.01[f]	–	0.236 ± 0.001[d]	–	25
oleoyl CoA	4.8 ± 0.06[f]	–	0.242 ± 0.002[d,f]	–	24
CoASH	6.04 ± 0.07[f]	0.05 ± 0.003	0.231 ± 0.002[c]	0.089 ± 0.002	25

[a] The anisotropy of tyrosine in L-FABP (2 μM) with or without 5-fold molar excess ligand was analyzed by a sum of exponentials as $r(t) = r(0)\sum g_i \exp(-t/\theta_i)$. [b] $\lambda_{exc} = 300$ nm; $\lambda_{em} = 341$ nm. [c] $r(0)$ was set to 0.32 (Lakowicz et al., 1987). [d] $r(0)$ was allowed to vary. [e] The "wobbling" cone angle was calculated for the L-FABP tyrosine on the basis of time-resolved fluorescence anisotropy data presented in the Table and by using the following equation: $r/r(0) = (3\cos^2 \phi - 1)/2$, where r is the residual (limiting) anisotropy, and $r(0)$is the sum of $r(0)g_1 + r(0)g_2$. The sum of $g_1 + g_2 = 1$. The $r(0)$ was set as 0.32, the fundamental anisotropy of *N*-acetyl-L-tyrosinamide in propylene glycol at −60 °C (Lakowicz et al., 1987). [f] $p < 0.05$ as compared to no ligand ($n = 5-6$).

Apo- and Holo-L-FABP Time-Resolved Anisotropy. Apo L-FABP anisotropy decay kinetics were biexponential. Long ($\theta_1 = 6.59$ ns) and fast components ($\theta_2 = 0.05$ ns) reflected overall protein motion and the average internal motions of Tyr residues in L-FABP, respectively (Table 5). Tyr segmental motion in apo-L-FABP (Table 5) was 8-fold faster than Trp segmental motion in apo-I-FABP (Table 3). The estimated "wobbling" cone angle, Φ, for Tyr rotations in apo-L-FABP was 25° (Table 5), 2.3-fold larger than for Trp in apo-I-FABP (Table 3). These data suggested remarkable rotational freedom of Tyr residues in the L-FABP protein globule.

Oleic acid significantly decreased the long correlation time, reflecting overall protein rotational dynamics, of L-FABP from 6.59 to 5.24 ns (Table 5). Under the same conditions, the short component was no longer resolvable, due possibly to even more rapid rotational motions of Tyr in the holo-L-FABP. The decrease of maximal anisotropy $r(0)$ for L-FABP from 0.32 to 0.236 (Table 5), which accompanied the loss of the short component, also indicated the presence of the fast depolarizing rotational motions consistent with this suggestion. Remarkably, the amplitude of Tyr fast rotational motions did not change as shown by the unaffected wobbling cone angle of 25° (Table 5). The addition of oleoyl CoA to the apo-L-FABP revealed the same pattern as did oleic acid addition: θ_1 decreased from 6.59 to 4.8 ns, and the rotational component indicating Tyr segmental mobility became too fast to be resolved. Concomitantly, oleoyl CoA reduced the I-FABP Tyr anisotropy parameter $r(0)$ [sum of $r(0)g_1 + r(0)g_2$] from 0.320 to 0.242 (Table 5). Again, the amplitude of Tyr rotation in the protein remained unchanged, wobbling cone angle of 24° (Table 5). CoASH elicited a small but significant effect on the overall rotation of L-FABP by lowering θ_1 from 6.59 to 6.04 ns (Table 5). However,

Table 6: Fluorescence Decay of *cis*-Parinaric Acid and Its CoA Derivative[a]

sample	τ_1 (ns)	τ_2 (ns)	τ_3 (ns)	f_1	f_2	f_3	$\tilde{\tau}$[b] (ns)
cis-PA in ethanol	1.99 ± 0.01	0.54 ± 0.04	–	0.95 ± 0.01	0.05 ± 0.01	–	1.95 ± 0.02
cis-PA/L-FABP	5.52 ± 0.19[c]	2.34 ± 0.07[c]	0.58 ± 0.08[c]	0.35 ± 0.03[c]	0.56 ± 0.03[c]	0.09 ± 0.01[c]	3.54 ± 0.08[c]
cis-PA/I-FABP	57.0[c]	4.56 ± 0.19[c]	1.15 ± 0.19[c]	0.20 ± 0.02[c]	0.48 ± 0.03[c]	0.32 ± 0.04[c]	14.2 ± 1.40[d,e]
cis-PA-CoA in ethanol	57.0	2.98 ± 0.04	1.37 ± 0.04	0.05 ± 0.006	0.40 ± 0.05	0.55 ± 0.05	4.50 ± 0.40[c]
cis-PA-CoA/L-FABP	57.0[e]	3.00 ± 0.07[c,e]	0.91 ± 0.03[d,e]	0.04 ± 0.006[e]	0.74 ± 0.003[d,e]	0.22 ± 0.003[d,e]	4.89 ± 0.32
cis-PA-CoA/I-FABP	58.3 ± 0.63	3.74 ± 0.40	1.07 ± 0.07	0.10 ± 0.01[f]	0.32 ± 0.09	0.58 ± 0.08[f]	7.59 ± 0.21[f,g]

[a] Fluorescence emission decay of *cis*-parinaric acid and its CoA derivative (each at 1 μM) in ethanol or bound to L-FABP or I-FABP (each at 2 μM) in buffer were analyzed by a sum of exponentials as $I(t) = \sum\alpha_i \exp(-t/\tau_i)$ where $\sum\alpha_i = 1$ and $f_i = \alpha_i\tau_i/\sum\alpha_i\tau_i$. The fraction of the light scatter for all samples was ≤0.02. All measurements were in PBS (pH 7.4) at 25 °C. [b] Mean fluorescence lifetime $\tilde{\tau}$ was calculated as $\tilde{\tau} = \sum f_i\tau_i$. [c] $p < 0.05$ as compared to *cis*-parinaric acid in ethanol ($n = 3-5$). [d] $p < 0.05$ as compared to *cis*-parinaroyl CoA in ethanol ($n = 3-5$). [e] $p < 0.05$ as compared to *cis*-parinaric acid bound to L-FABP ($n = 3-5$). [f] $p < 0.05$ as compared to *cis*-parinaric acid bound to I-FABP ($n = 3-5$). [g] $p < 0.05$ as compared to *cis*-parinaroyl CoA bound to L-FABP ($n = 3-5$).

CoASH did not alter the rapid rotation or the wobbling cone angle of L-FABP Tyr, 25° (Table 5).

Fluorescence Properties of cis-Parinaric Acid and cis-Parinaroyl CoA Interacting with Holo-I-FABP and Holo-L-FABP

cis-Parinaric Acid and cis-Parinaroyl CoA Steady-State Fluorescence. Although *cis*-parinaric acid is monomeric in ethanol, it absorbs poorly in water, due possibly to formation of dimers (Hudson et al., 1986; Nemecz et al., 1991a,b). Likewise, titration of L-FABP with *cis*-parinaroyl CoA in aqueous buffer increased fluorescence emission with maxima at 292, 307, and 322 nm (Figure 6A). These maxima were red-shifted by about 3 nm as compared to those in ethanol. This increase in *cis*-parinaroyl CoA absorbance was accompanied by an increase in fluorescence intensity with maximum emission near 420 nm (Figure 6B). The same pattern in both absorbance and emission spectra of *cis*-parinaroyl CoA was observed when I-FABP was titrated (data not shown).

cis-Parinaric Acid Fluorescence Emission Decay. Analysis of *cis*-parinaric acid fluorescence decay in absolute ethanol revealed mostly monoexponential decay with the major lifetime component of $\tau = 1.99$ ns accounting for 95% of the fatty acid emission (Table 6). The mean lifetime was calculated to be 1.95 ns and was typical of that of reported earlier for the *cis*-parinaric acid and other compounds of polyenic structure in alcohol solvents (Wolber & Hudson, 1981; Bondarev & Bachilo, 1991). In aqueous buffers, *cis*-parinaric acid readily forms aggregates thereby precluding detection of its monomeric fluorescence decay. In the presence of L-FABP *cis*-parinaric acid emission decay was best fit to three components. The major lifetime component, $\tau_2 = 2.34$ ns, accounted for 56% of fatty acid emission, resulting in a mean lifetime of 3.54 ns (Table 6). The same fatty acid also displayed three-exponential fluorescence decay kinetic when it was bound to I-FABP (Table 6). In contrast to L-FABP, *cis*-parinaric acid associated with I-FABP showed the presence of a very long component $\tau_1 \approx 50$ ns. This value should probably considered as a low limit for τ_1, because the best fit of the *cis*-parinaric acid emission decay curve ($\chi^2 < 3$) was obtained when this parameter was fixed at 57 ns. When this parameter was allowed to vary, the resultant analysis yielded inconsistent τ_1 values ranging from 57 to about 1000 ns for the different decay curves, without significant effect on either τ_2 and τ_3 values or their fractions (data not shown). The mean fluorescence lifetime for the *cis*-parinaric acid associated with I-FABP was 14.2 ns (Table 6), 3.6-fold longer than the average lifetime of *cis*-parinaric acid bound to L-FABP.

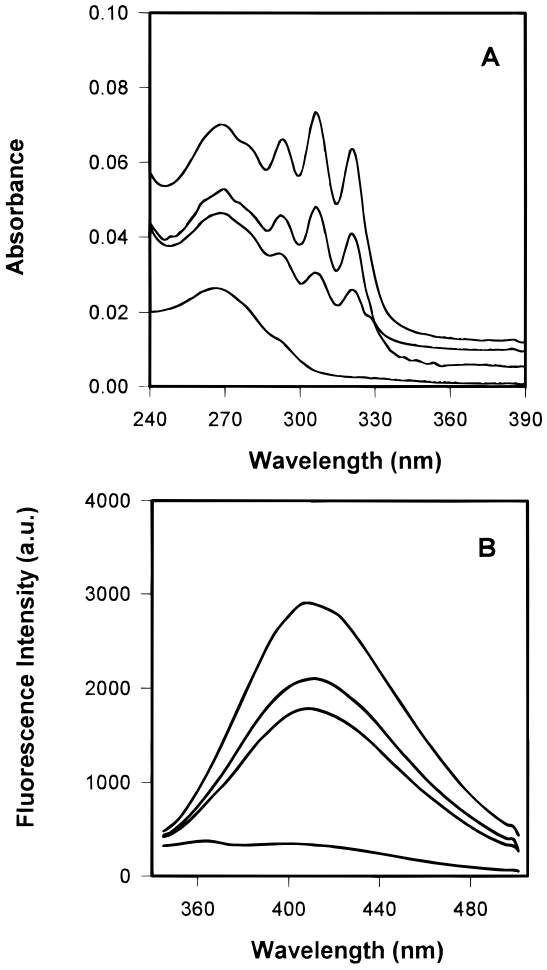

FIGURE 6: Spectral characteristics of *trans*-parinaric acid upon its interaction with L-FABP. (A) absorption spectra of *trans*-parinaroyl CoA upon its binding to L-FABP. From bottom to top: L-FABP only (1.15 μM); L-FABP + 0.13 μM *trans*-parinaroyl CoA; L-FABP + 0.26 μM *trans*-parinaroyl CoA; L-FABP + 0.40 μM *trans*-parinaroyl CoA, and L-FABP + 0.53 μM *trans*-parinaroyl CoA. (B) Uncorrected fluorescence emission spectra of *trans*-parinaroyl CoA with excitation at 310 nm. From bottom to top: 1.15 μM L-FABP + 0.13 μM *trans*-parinaroyl CoA; 1.15 μM L-FABP + 0.26 μM *trans*-parinaroyl CoA; 1.15 μM L-FABP + 0.40 μM *trans*-parinaroyl CoA, and 1.15 μM L-FABP + 0.53 μM *trans*-parinaroyl CoA.

cis-Parinaroyl CoA Fluorescence Emission Decay. As observed for *cis*-parinaric acid, fluorescence emission decay of *cis*-parinaroyl CoA in ethanol also showed three lifetime components. However, the *cis*-parinaroyl CoA in ethanol lifetime components [57 ns (fraction 0.05); 1.37 ns (fraction 0.55); and 2.98 ns (fraction 0.40)] differed substantially in the value of each lifetime as well as its associated fraction

Table 7: Anisotropy Decay of *cis*-Parinaric Acid and *cis*-Parinaroyl CoA Bound to L-FABP and I-FABP[a]

protein	ligand	θ_1 (ns)[b]	θ_2 (ns)	r_0g_1[c]	r_0g_2	"wobbling" cone angle (deg)[d]
L-FABP	*cis*-PA	8.23 ± 0.15	–	0.358 ± 0.005	–	13
	cis-PA-CoA	10.7 ± 0.40[e]	–	0.388 ± 0.010[e]	–	3
I-FABP	*cis*-PA	6.25 ± 0.50[e]	0.218 ± 0.007[e]	0.257 ± 0.015[e]	0.143 ± 0.015[e]	29
	cis-PA-CoA	5.95 ± 0.50[g]	0.090 ± 0.010[f,g]	0.230 ± 0.020[g]	0.170 ± 0.020[g]	32

[a] All conditions were as described in the legend to Table 6 except that anisotropy decay of the fatty acid or fatty acyl CoA bound to protein was analyzed by a sum of exponentials as $r(t) = r(0)\sum g_i \exp(-t/\theta_i)$. [b] $\lambda_{exc} = 325$ nm; $\lambda_{em} \geq 370$ nm. [c] $r(0)$ was allowed to vary. [d] Wobbling cone angle was calculated as in Table 5. [e] $p < 0.05$ vs *cis*-parinaric acid bound to L-FABP ($n = 5-6$). [f] $p < 0.05$ vs *cis*-parinaric acid bound to I-FABP ($n = 5-6$). [g] $p < 0.05$ vs *cis*-parinaroyl CoA bound to L-FABP ($n = 5-6$).

as compared to *cis*-parinaric acid in ethanol (Table 6). Consequently, the mean lifetime of *cis*-parinaroyl CoA in ethanol, 4.5 ns, was significantly higher than that of 1.92 ns for *cis*-parinaric acid in ethanol (Table 6). The reason for difference in fluorescence decay between *cis*-parinaric acid and *cis*-parinaroyl CoA in absolute alcohol is not known. Despite its higher solubility in aqueous buffer, the extremely low fluorescent quantum yield of *cis*-parinaroyl CoA in aqueous buffer prohibited measurement of monomeric *cis*-parinaroyl CoA time-resolved fluorescence. The association of *cis*-parinaroyl CoA with L-FABP altered the fluorophore decay kinetics (as compared to those in ethanol) such that τ_3 decreased from 1.37 to 0.91 ns and the τ_2 fraction increased from 0.40 to 0.74 at expense of the shortest-lifetime component (Table 6). As a result, the mean lifetime in of L-FABP-bound *cis*-parinaroyl CoA was slightly increased from 4.5 to 4.89 ns (Table 6). In contrast, interaction of *cis*-parinaroyl CoA with I-FABP did not significantly affect the lifetime values but redistributed their fractions (Table 6). The fractions of τ_1 and τ_3 were almost doubled at expense of the second component and increased the mean lifetime from 4.50 to 7.59 ns (Table 6).

cis-Parinaric Acid Time-Resolved Anisotropy. Anisotropy decay kinetics of L-FABP-bound *cis*-parinaric acid were monoexponential, yielding a single rotational correlation time of 8.23 ns (Table 7). The apparent lack of a rapid segmental mobility component, θ_2, could be due either to this motion being too rapid to be measured or to the ligand being held very tightly in the L-FABP binding site. However, the fact that the measured maximal anisotropy $r(0)g_1 = 0.358$ was less than the static (fundamental) fluorescence anisotropy (r_o) reported earlier for the same fatty acid in a propylene glycol glass, $r_o = 0.39$ (Wolber & Hudson, 1981) was consistent with the *cis*-parinaric acid rotating rapidly in the L-FABP matrix. The amplitude of such rotational motions was estimated to be 13° (Table 7). Hence, the measured long rotational correlation time, θ_1, primarily represents the characteristics of the overall rotational dynamics of the L-FABP globule. In contrast to L-FABP, anisotropy decay of *cis*-parinaric acid bound to I-FABP displayed multiexponential kinetics with both long and short rotational correlation times, 6.25 and 0.218 ns, respectively (Table 7). Again, the long rotational component can be assigned to the overall rotation of the protein, while the short component reflects fast rotational motions of the *cis*-parinaric acid inside the I-FABP binding site. The measured limiting anisotropy of I-FABP-bound *cis*-parinaric acid, $r(0)g_1 = 0.218$, was much less than that of L-FABP-bound *cis*-parinaric acid. This is consistent with *cis*-parinaric acid having greater rotational motion in the I-FABP binding site as compared to the L-FABP binding site. The estimated wobbling cone angle of 29° for *cis*-parinaric acid bound to I-FABP is in support of the above observation.

cis-Parinaroyl CoA Time-Resolved Anisotropy. Anisotropy decay of *cis*-parinaroyl CoA bound to L-FABP also exhibited single exponential decay, reflecting the overall rotation of the protein with correlation time of 10.7 ns, significantly higher than that obtained with *cis*-parinaric acid 8.2 ns (Table 7). The maximal anisotropy for *cis*-parinaroyl CoA in L-FABP was 0.388, also higher than that obtained for *cis*-parinaric acid bound to L-FABP value (Table 7). The latter is consistent with *cis*-parinaroyl CoA being almost completely immobilized in the L-FABP matrix, wobbling cone angle 3° (Table 7). *cis*-Parinaroyl CoA bound to I-FABP displayed multiexponential rotational dynamics with long and short components, 5.95 and 0.09 ns (Table 7). It should be noted that *cis*-parinaroyl CoA interacting with I-FABP underwent very fast rotational motion, as is shown by its respective correlation time 0.09 ns (Table 7). This fast motion was faster than that observed for *cis*-parinaric acid bound to I-FABP (and faster than either ligand bound to L-FABP). This observation is consistent with the fact that the maximal anisotropy $r(0)g_1 = 0.230$ is much less than the static (fundamental) anisotropy $r_o = 0.400$. This strongly indicates the existence of fast rotational motions of the *cis*-parinaroyl CoA molecule inside I-FABP. The amplitude of such motions was estimated to be 32° (Table 7).

Orientation of Fatty Acid Bound to L-FABP and I-FABP

As pointed out in the introduction, it is thought that the orientation of fatty acids bound to L-FABP and I-FABP is opposite, i.e., fatty acid carboxyl facing outward in L-FABP (solution NMR data) and fatty acid carboxyl facing deep into the binding pocket of I-FABP (X-ray crystallography data). This possibility was examined by using a *cis*-parinaric acid displacement assay with two different displacing ligands: (i) A monocarboxylic fatty acid (hexadecanoic acid, i.e., palmitic acid) which could bind either with the methyl end or the carboxyl end buried in the protein binding pocket; (ii) dicarboxylic acid (hexadecanedioic acid, i.e., thapsic acid) which can only bind with a carboxyl facing deep into the binding pocket. *cis*-Parinaric acid, bound to I-FABP, was displaced with hexadecanedioic acid (thapsic acid) and with hexadecanoic acid (16:0, palmitic acid) nearly equally at all three concentrations tested (Figure 7B). Likewise, *cis*-parinaric acid bound to L-FABP was displaced with both hexadecanedioc acid (thapsic acid) and with hexadecanoic acid (16:0, palmitic acid) (Figure 7A). However, the dicarboxylic thapsic acid was nearly twice as effective in displacing L-FABP-bound *cis*-parinaric acid than was the monocarboxylic palmitic acid. These results are consistent with the fatty acid bound I-FABP with the carboxyl buried in the interior of the binding site. Furthermore, the displacement data suggest that fatty acids may also bind to L-FABP with the carboxyl end buried in the interior.

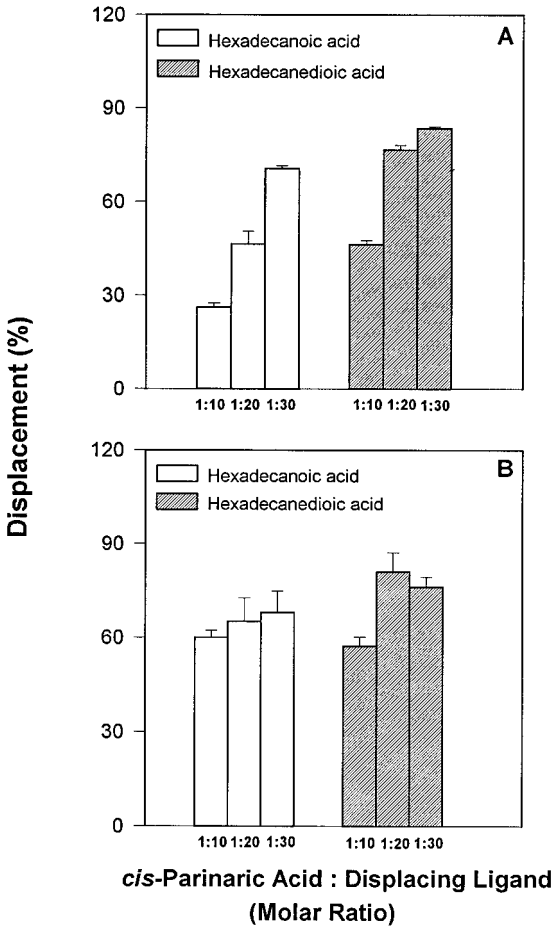

FIGURE 7: Displacement of *cis*-parinaric acid bound to L-FABP (panel A) and I-FABP (panel B) by hexadecanoic (palmitic) and hexadecanedioic (thapsic) acids. Protein concentration was 0.15 μM; *cis*-parinaric acid concentration was 0.45 μM. Excitation and emission wavelengths were 310 and 416 nm, respectively.

DISCUSSION

Despite in-depth crystallographic analysis of many members of the fatty acid binding protein family (reviewed in Banaszak et al. (1994) and Sacchettini and Gordon (1993)], our understanding of the hydrodynamic properties and conformations of these proteins, especially the L-FABP, is limited. Even less is known regarding the effects of different ligands on these parameters for I-FABP and I-FABP in solution. The studies presented herein utilized time-resolved and steady-state fluorescence techniques to provide new insights on the conformation of I-FABP and L-FABP in solution and on the effects of several ligands on these conformations.

First, time-resolved fluorescence studies show that ligand binding altered I-FABP conformation by increasing the I-FABP Trp wobbling cone angle as much as 2.5-fold in the following order: oleoyl CoA > CoASH > oleic acid > no ligand. While these ligands did not alter the L-FABP Tyr wobbling cone angle, it must be noted that the Trp and Tyr residues do not appear to be in conserved regions of both proteins. Thus, on the basis of Trp and Tyr properties alone, it is not possible to make direct comparisons and conclude that ligands affect the conformation of I-FABP but not L-FABP.

Second, time-resolved anisotropy studies presented herein demonstrate that fatty acids and fatty acyl CoAs differentially alter the hydrodynamic properties of the entire L-FABP and I-FABP protein molecules in solution. The overall rotational time of I-FABP, 6.57 ns, was not significantly different from that of L-FABP, 6.59 ns. This observation is consistent with the similarity in molecular weights of these proteins and suggests that their overall shape in solution may also be similar. None of the ligands tested altered the overall hydrodynamic properties of I-FABP. This conclusion is in agreement with X-ray crystallographic data showing that fatty acid binding did not alter the tertiary structure of I-FABP (Banaszak et al., 1994; Sacchettini & Gordon, 1993). In contrast, upon interacting with L-FABP all three ligands (oleoyl CoA, oleic acid, and CoASH) significantly decreased the protein overall rotational time, θ_1, such that the motion of the entire L-FABP protein appeared as much as 27% faster upon ligand binding (Table 5). In any case, ligand binding altered not only the local environment and dynamics of Tyr in L-FABP but also the rotational correlation time of the protein as a whole. The latter suggests significant solution conformational changes in the L-FABP upon ligand binding. These observations are also in agreement with early reports that addition of native fatty acids may alter L-FABP aromatic acid fluorescence emission, indicating conformational changes in the L-FABP upon fatty acid binding (Nemecz et al., 1991b; Trotter & Storch, 1989). Furthermore, second-derivative absorption spectroscopy of FABP aromatic amino acids also showed that fatty acid binding altered the conformation of L-FABP but not I-FABP (Nemecz et al., 1991b). Other fluorescence studies also suggested conformational changes in the FABPs upon fatty acyl CoA binding (Wilton, 1989; Evans & Wilton, 1990; Thumser & Wilton, 1994). For example, oleoyl CoA increased the reactivity of L-FABP Cys to DTNB (even though it may be remote from the fatty acid binding site), increased fluorescence of L-FABP Cys reacted with AEDANS, and decreased fluorescence emission of a variety of L-FABP mutants in which Trp was inserted into the structure. Additional details of I-FABP and L-FABP folding with or without bound ligands are based on studies utilizing infrared (Muga et al., 1993), fluorescence, and circular dichroism (Ropson et al., 1990; Cistola et al., 1989; Jolly et al., submitted) spectroscopy to examine effects of pH, detergent, or temperature on protein denaturation. The basic conclusions from these studies are (i) fatty acid binding did not change the overall basic structural features of the FABP, i.e., the proportion of helix, β-sheet, and random coil in the L-FABP or I-FABP structure remained constant; (ii) fatty acid binding stabilized the FABP structures in some unknown way and made the FABP proteins more resistant to temperature or pH induced unfolding; (iii) Data with another member of the FABP superfamily, cellular retinoic acid binding protein, showed that ligand binding protected the protein from limited proteolysis (Jamison et al., 1994). This suggests that a ligand-induced conformational change is occurring in this protein (Jamison et al., 1994). The data presented herein with time-resolved protein fluorescence spectroscopy provide a substantive basis for this initial suggestion and furthermore show that not only fatty acids but also fatty acyl CoAs and/or CoASH can alter hydrodynamic conformational properties of L-FABP, but not I-FABP, in solution. While the data are consistent with CoASH binding/interacting with both I-FABP and L-FABP, this interaction appeared to be stronger/less loose with L-FABP thereby eliciting hydrodynamic changes in L-FABP. While CoASH did not alter the overall hydrodynamic properties of I-FABP, it still decreased the local segmental order of I-FABP Trp (Table 3). However, a specific CoASH binding

site has not been identified in either L-FABP or I-FABP at this time. In the case of acyl CoA binding protein (ACBP), a specific site in the protein interacts with the CoASH portion of fatty acyl CoAs, but apparently not with free CoASH [reviewed in Gossett et al. (1996)]. The observations with the presence of subtle structure changes in I-FABP upon ligand binding are consistent with X-ray crystallography of apo- and holo-I-FABPs in which fifteen amino acids are located within 4.1 Å of the bound fatty acid (Sacchettini et al., 1989). These include Tyr-14, Tyr-117, and Trp-82. Of the fifteen amino acids close to the bound fatty acid, only Ala-73 showed any significant main chain movement in the crystalline holo-I-FABP. Additional, more subtle X-ray crystal based conformational dissimilarities in the holo- vs apo-I-FABP were restricted to side chains of Ile-23, Ala-73, and Asp-74 in the binding pocket interior and Arg-56 and Lys-27 in the fatty acid "entry portal". However, similar molecular details for apo- and holo-L-FABP crystal structure are not yet available.

Third, fluorescent fatty acids and fatty acyl CoAs were used to examine the polarity of the I-FABP and L-FABP ligand binding sites. Numerous fluorescent fatty acids have been used extensively to explore the polarity of I-FABP and L-FABP fatty acid binding sites (Hubbell et al., 1994; Nemecz et al., 1991a,b; Richieri et al., 1994, 1992; Schulenberg-Schell et al., 1988; Storch et al., 1989; Trotter & Storch, 1989). Absorbance spectral shifts and ratios of fluorescence excitation maxima of *cis*-parinaric acid suggested that the microenvironment of the I-FABP fatty acid binding site was much less polar than that of L-FABP (Nemecz et al., 1991b): I-FABP and L-FABP fatty acid binding site apparent dielectric constants were 16 and 30, respectively (Nemecz et al., 1991b). The mean lifetime of *cis*-parinaric acid in hydrophobic solvents such as cyclohexanol was much longer than in more polar solvents such as ethanol (Parasassi et al., 1984). Consistent with these observations, the mean lifetime of *cis*-parinaric acid bound to I-FABP was 3.6-fold longer than bound to L-FABP (Table 6) and confirmed the lower polarity of the I-FABP fatty acid binding site. In contrast, nothing is known regarding the polarity of the fatty acyl CoA binding sites in the respective I-FABP and L-FABP binding pockets. Table 6 shows that the mean lifetime of I-FABP-bound *cis*-parinaroyl CoA was 1.6-fold longer than that bound to L-FABP. In summary, fluorescence lifetime data of FABP-bound *cis*-parinaric acid and *cis*-parinaroyl CoA suggest that the microenvironment of the I-FABP ligand binding site is much less polar than that of L-FABP.

Fourth, fluorescent fatty acids and fatty acyl CoAs were used to examine the environment of the I-FABP and L-FABP ligand binding sites. Although numerous fluorescent fatty acids have been used extensively to explore the polarity of I-FABP and L-FABP fatty acid binding sites (Hubbell et al., 1994; Nemecz et al., 1991a,b; Richieri et al., 1992, 1994; Schulenberg-Schell et al., 1988; Storch et al., 1989; Trotter & Storch, 1989), much less is known regarding rotational dynamics of the ligands in the binding pocket. Therefore, fluorescent *cis*-parinaric acid and *cis*-parinaroyl CoA were used to provide additional molecular details of ligand motional dynamics within the L-FABP and I-FABP ligand binding sites. Such motions are not resolvable through crystallographic studies. Anisotropy decay analysis of fluorescent ligands bound to I-FABP and L-FABP resolved major differences sensed by the ligand in the binding sites of these proteins. The maximal anisotropy of *cis*-parinaric acid *cis*-parinaroyl CoA in L-FABP, 0.358 and 0.388, indicated that these ligands were very ordered within the L-FABP binding site. Their respective wobbling cone angles were 13° and 3°, respectively. In contrast, the same ligands were much less restricted within the I-FABP binding site(s) with significantly lower maximal anisotropies resulting in wobbling cone angles of 29° and 32°, respectively. The rotational correlation time θ_1 of *cis*-parinaric acid *cis*-parinaroyl CoA in L-FABP, 8.23 and 10.7 ns, was significantly longer than that obtained with L-FABP Tyr, 6.59 ns, suggesting that the orientation of these ligands in the binding site was along a longer axis and that L-FABP may be ellipsoid or "clam" shaped. The clam shape is suggested by the fact that the crystal structures of all the other known FABPs is also clam shaped and that low-resolution X-ray crystallography of L-FABP from chicken liver is also consistent with such a shape [reviewed in Banaszak et al. (1994)]. The rotational correlation time θ_1 of *cis*-parinaric acid *cis*-parinaroyl CoA in I-FABP, 6.25 and 5.95 ns, was essentially the same as that obtained with I-FABP Trp, 6.57 ns, indicating that the orientation of these ligands in the binding site was more along the long axis of an ellipsoid or clam shaped L-FABP. The clam shape is suggested by the fact that the crystal structures of all the other known FABPs are also clam shaped (Banaszak et al., 1994; Sacchettini & Gordon, 1993). In summary, the ligand binding sites of I-FABP and L-FABP differ markedly in the degree to which they order both the fatty acids and the fatty acyl CoAs.

Fifth, the data presented herein contribute to resolution of the orientation of fatty acids and other ligands in the binding sites of I-FABP vs L-FABP. Three common themes are evident from crystallographic analyses of FABP structure [reviewed in Banaszak et al., (1994)]. (i) With the possible exception of L-FABP these proteins have nearly superimposable crystal structures with only subtle differences apparent. Although the reported X-ray crystal structure of L-FABP is less clear than those of the other FABPs, it appears consistent with the above trend. (ii) With the possible exception of L-FABP, all of the FABPs appear to bind fatty acids with the fatty acid carboxylate buried deep in the FABP binding pocket and interacting with a basic residue such as Arg. (iii) In the holo-FABPs the presence of bound fatty acid does not significantly alter the tertiary crystal structure. In contrast to this well-developed X-ray crystallographic picture of fatty acid interaction with most FABPs, much less is known of the solution structure of L-FABP and the orientation of fatty acids and other ligands on the solution conformation of these proteins. Two studies utilizing NMR techniques investigated the orientation of ^{13}C-fatty acids within the fatty acid binding sites of I-FABP and L-FABP in solution (Cistola et al., 1988,1989). On the basis of the pH titratability of the ^{13}C-carboxyl-labeled fatty acids bound to these FABPs, the basic conclusion of the NMR studies was that bound fatty acids were oriented oppositely in the respective FABP binding pockets: with fatty acyl carboxyl groups exposed at the protein surface and accessible to pH titration (L-FABP) or with fatty acyl carboxyl group buried deep in the protein interior and inaccessible to pH titration (I-FABP) (Cistola et al., 1988, 1989). Thus, L-FABP appeared to be an exception to a basic rule followed by all the other FABPs, namely, that the fatty acid carboxylate was buried in the fatty acid interior. (iv) Several observations are not consistent with such an orientation of

fatty acids in L-FABP: L-FABP-bound *cis*-parinaric acid was displaced with the dicarboxylic acid, hexadecanedioc acid (thapsic acid), as well as with hexadecanoic acid (16:0, palmitic acid) (Figure 7). Also, Silicon Graphics modeling of L-FABP indicates that the interior of this protein fatty acid binding pocket does contain several amino acid residues that might interact with a fatty acid carboxyl (Schroeder et al., 1993). (v) L-FABP binds two fatty acids, unlike I-FABP which binds only one fatty acid. Induced circular dichroism of bound *cis*-parinaric acid has been used to suggest the presence of a single L-FABP binding site that binds two fatty acids within that site (Keuper et al., 1985). If these fatty acids were both oriented in parallel within this binding site they would be expected to self-quench. However, as described herein and earlier (Keuper et al., 1985; Nemecz et al., 1991a,b) *cis*-parinaric acid did not self-quench even when two *cis*-parinaric acids bound per molecule of L-FABP. This observation could be explained either by antiparallel orientation of two fatty acids within a single fatty acid binding site or by the presence of two separate fatty acid binding sites in L-FABP. (vi) It has been suggested that the dominant structural feature accounting for the high affinity of fatty acids to FABPs appears to be the ionic interaction between the fatty acid carboxylate and a basic amino acid residue in the fatty acid binding pocket (Banaszak et al., 1994; Sacchettini et al., 1989). Thus, one might expect I-FABP (with its fatty acyl carboxyl forming ionic interactions with Arg deep in the binding pocket) to have a higher affinity for fatty acid than L-FABP. According to the NMR data (Cistola et al., 1988, 1989), L-FABP has a titratable fatty acyl carboxyl at the surface of the protein. Yet, L-FABP and I-FABP have very similar affinities for fatty acids (Lowe et al., 1984; Nemecz et al., 1991a). Furthermore, when recombinant I-FABP and recombinant L-FABP are isolated from the same strain of bacteria, both proteins contain endogenous bound fatty acids: L-FABP, 1.6 mol of fatty acids/mol protein (80% occupancy of available sites); I-FABP, 0.7 mol of fatty acids/mol of protein (70% occupancy of available sites) (Lowe et al., 1984). (vii) Chemical modification of the interior Arg-122 of bovine L-FABP reduced fatty acid binding by 60% (Schulenberg-Schell et al., 1988). Silicon Graphics modeling of L-FABP on the I-FABP α-carbon backbone showed that this Arg residue is located deep in the fatty acid binding pocket in a region near where Arg-106 is located in I-FABP (Schroeder et al., 1993). (viii) L-FABP has a 20-fold higher affinity for fatty acids (*cis*-parinaric acid) than the fatty acyl CoA derivative of the fatty acid (*cis*-parinaroyl CoA) (Schroeder et al., 1993; Hubbell et al., 1994; Nemecz et al., 1991a). Yet, both ligands bind at the same binding sites. If the fatty acid bound with the methyl end buried in the interior of the L-FABP, then one might expect a similar degree/affinity of fatty acyl CoA binding. The methyl end of the fatty acyl CoA is equally available for insertion deep into the interior of a putative L-FABP binding pocket. (ix) While there is no doubt that NMR analysis of carboxyl ^{13}C-labeled fatty acid binding to L-FABP showed this carboxyl to be pH titratable in L-FABP (but not I-FABP), this interpretation of this observation is based on a lack of structural changes in the FABP upon pH titration. Indeed, circular dichroism data showed that the tertiary structure of I-FABP was unresponsive to pH titration (Cistola et al., 1988, 1989). In contrast, circular dichroism data showed that the tertiary structure of L-FABP unfolded concomitant with pH titratability of the carboxyl ^{13}C-labeled fatty acid bound to L-FABP (Cistola et al., 1988, 1989). This suggests an alternate explanation for the NMR data with L-FABP: perhaps pH-induced protein unfolding increased access of the interior of the L-FABP to protons such that a fatty acid carboxylate bound deep in the binding pocket might become titratable. If this were so, then L-FABP would bind fatty acids with the carboxylate buried in the interior of the protein, just like the other FABPs.

Elucidation of how fatty acids and fatty acyl CoAs bind to FABPs is important to our understanding how these proteins may function in cells. Both fatty acids and fatty acyl CoAs are important ligands as precursors of larger macromolecules including triglycerides, glycerides, phospholipids, plasmalogens, cholesteryl esters, etc. In addition, fatty acids and fatty acyl CoAs are also important for activating enzymes (protein kinase C), signaling, regulation of gene transcription, etc. (Gossett et al., 1996). Binding of fatty acids and fatty acyl CoAs to cytosolic FABPs may thereby modulate the activities of the fatty acids and fatty acyl CoAs (Gossett et al., 1996). Finally, enzymes or processes affected by these ligands may be influenced differentially by the FABP-bound form of the ligand as compared to the free form of the ligand. For example, prior dissociation of the ligand from retinol binding protein is not required by microsomal lecithin−retinol acyl transferase (Herr & Ong, 1992). Furthermore, the latter enzyme discriminates between apo- and holo-binding protein (Herr & Ong, 1992). Likewise, the transcription factor Fad R requires binding of fatty acyl CoA to induce a conformational change in Fad R, thereby conferring DNA binding ability and transcriptional regulatory activity to Fad R (DiRusso et al., 1992). Proteins such as L-FABP or I-FABP as well as other fatty acyl CoA binding proteins may regulate the concentration of free fatty acyl CoA available for transcriptional proteins binding fatty acyl CoAs (Gossett et al., 1996).

In summary, the data presented herein provide new insights on the conformation of I-FABP and L-FABP in solution. It was shown that ligands such as fatty acyl CoA, fatty acids, and/or CoASH differentially affected not only the local segmental motions of the FABP peptide chains but also the hydrodynamic properties of the entire FABP molecules. Moreover, the degree of motional restraint and/or dynamics of fluorescent fatty acids and/or fatty acyl CoAs differed markedly within the binding sites of these proteins. Finally, studies with dicarboxylic acids provided new understanding on the potential orientation of these ligands within the binding sites of I-FABP and L-FABP.

REFERENCES

Baier, L. J., Sacchettini, J. C., Knowler, W. C., Eads, J., Paolisso, G., Tataranni, P. A., Mochizuki, H., Bennett, P. H., Bogardus, C., & Prochazka, M. (1995) *J. Clin. Invest. 95*, 1281.

Banaszak, L., Winter, N., Xu, Z., Bernlohr, D. A., Cowan, S., & Jones, T. A. (1994) *Adv. Protein Chem. 45*, 89.

Bass, N. M. (1988) *Int. Rev. Cytol. 111*, 143.

Bondarev, S. L., & Bachilo, S. M. (1991) *J. Photochem. Photobiol. A: Chem, 59*, 273.

Bradford, M. (1976) *Anal. Biochem. 72*, 248.

Burstein, E. A., Vedenkina, N. S., & Ivkova, M. N. (1973) *Photochem. Photobiol. 18*, 263.

Cantor, C. R., & Schimmel, P. R. (1980) in *Biophysical Chemistry*, W. H. Freeman & Co., San Francisco, CA.

Cistola, D. P., Walsh, M. T., Corey, R. P., Hamilton, J. A., & Brecher, P. (1988) *Biochemistry 27*, 711.

Cistola, D. P., Sacchettini, J. C., Banaszak, L. J., Walsh, M. T., & Gordon, J. I. (1989) *J. Biol. Chem. 264*, 2700.
Demchenko, A. P. (1986) in *Ultraviolet Spectroscopy of Proteins*, Springer-Verlag, Berlin, Heidelberg.
DiRusso, C. C., Heimert, T. L., & Metzger, A. K. (1992) *J. Biol. Chem. 267*, 8685.
Elofsson, A., Rigler, R., Nilsson, L., Roslund, J., Krause, G., & Holmgren, A. (1991) *Biochemistry 30*, 9648.
Evans, C., & Wilton, D. C. (1990) *Mol. Cell. Biochem. 98*, 135.
Glatz, J., & Veerkamp, J. (1983) *Anal. Biochem 132*, 89.
Glatz, J. F., & Veerkamp, J. H. (1985) *Int. J. Biochem. 17*, 13.
Gordon J. I., & Lowe, J. B. (1985) *Chem. Phys. Lipids 38* (1−2), 137.
Gossett, R. E., Frolov A. A., Roths, J. B., Behnke, W. D., Kier, A. B., & Schroeder, F. (1996) *Lipids 31*, 895.
Herr, F. M., & Ong, D. E. (1992) *Biochemistry 31*, 6748.
Hubbell, T., Behnke, W. D., Woodford, J. K., & Schroeder, F. (1994) *Biochemistry 33*, 3327.
Hudson, B. S., Harris, D. L., Ludescher, R. D., Ruggiero, A., Cooney-Freed, A., & Cavalier, S. A. (1986) Fluorescence Probe Studies of Proteins and Membranes, in *Applications of Fluorescence in the Biomedical Sciences* (Taylor, D. L., Waggoner, A. S., Murphy, R. F., Lanni, F., & Birge, R. R., Eds.) p 159, Alan R. Liss Inc., New York.
Jakoby, M. G., Miller, K. R., Toner, J. J., Bauman, A., Cheng, L., Li, E., & Cistola, D. P. (1993) *Biochemistry 32*, 872.
Jamison, R. S., Newcomer, M. E., & Ong, D. E. (1994) *Biochemistry 33*, 2873.
Jefferson, J. R., Slotte, J. P., Nemecz, G., Pastuszyn, A., Scallen, T. J., & Schroeder, F. (1991) *J. Biol. Chem. 266*, 5486.
Jolly, C. A., Hubbell, T., Behnke, W. D., & Schroeder, F. (1996) *Arch. Biochem. Biophys.* (submitted).
Kaikaus, R. M., Bass, N. M., & Ockner, R. K. (1990) *Experientia 46*, 617.
Kanda, T., Odani, S., Tomoi, M., Matsubara, Y., & Ono, T. (1991) *Eur. J. Biochem. 197*, 759.
Keuper, H. J., Klein, R. A., & Spener, F. (1985) *Chem. Phys. Lipids 38*, 159.
Lakowicz, J. R., Maliwal, B. P., Cherek, H., & Batler, A. (1983) *Biochemistry 22*, 1741.
Lakowicz, J. R., Laczko, G., & Gryczynski, I. (1987) *Biochemistry 26*, 82.
Lipari, G., & Szabo, A. (1980) *Biophys. J. 30*, 489.
Lowe, J. B., Strauss, A. W., & Gordon, J. I. (1984) *J. Biol. Chem. 259*, 12696.
Lowe, J. B., Sacchettini, J. C., Laposata, M., McQuillan, J. J., & Gordon, J. I. (1987) *J. Biol. Chem. 262*, 5931.
Miller, K. R., & Cistola, D. P. (1993) *Mol. Cell. Biochem. 123*, 29.
Muga, A., Cistola, D. P., & Mantsch, H. H. (1993) *Biochim. Biophys. Acta 1162*, 291.
Nemecz, G., Hubbell, T., Jefferson, J. R., Lowe, J. B., & Schroeder, F. (1991a) *Arch. Biochem. Biophys. 286*, 300.
Nemecz, G., Jefferson, J. R., & Schroeder, F. (1991b) *J. Biol. Chem. 266*, 17112.
Parasassi, T., Conti, F., & Gratton, E. (1984) *Biochemistry 23*, 5660.
Paulussen, R. J. A., & Veerkamp, J. H. (1990) *Subcell. Biochem. 16*, 175.
Prows, D. R., Murphy, E. J., & Schroeder, F. (1995) *Lipids 30*, 907.
Prows, D. R., Murphy, E. J., Moncecchi, D., & Schroeder, F. (1996) *Chem. Phys. Lipids 84*, 47−56.
Pryde, E. H. (1979) in *Fatty Acids*, The American Oil Chemist's Society, Champaign, IL.
Rasmussen, J. T., Börchers, T., & Knudsen, J. (1990) *Biochem. J. 265*, 849.
Richieri, G. V., Ogata, R. T., & Kleinfeld, A. M. (1992) *J. Biol. Chem. 267*, 23495.
Richieri, G. V., Ogata, R. T., & Kleinfeld, A. M. (1994) *J. Biol. Chem. 269*, 23918.
Rolf, B., Oudenampsen-Kruger, E., Borchers, T., Faergeman, N. J., Knudsen, J., Lezius, A., & Spener, F. (1995) *Biochim. Biophys. Acta. 1259*, 245.
Ropson, I. J., Gordon, J. I., & Frieden, C. (1990) *Biochemistry 29*, 9591.
Sacchettini, J. C., & Gordon, J. I. (1993) *J. Biol. Chem. 268*, 18399.
Sacchettini, J. C., Gordon, J. I., & Banaszak, L. J. (1989) *J. Mol. Biol. 208*, 327.
Schroeder, F., Jefferson, J. R., Powell, D., Incerpi, S., Woodford, J. K., Colles, S. M., Myers-Payne, S., Emge, T., Hubbell, T., Moncecchi, D., Prows, D. R., & Heyliger, C. E. (1993) *Mol. Cell. Biochem. 123*, 73.
Schulenberg-Schell, H., Schafer, P., Keuper, H. J., Stanislawski, B., Hoffmann, E., Ruterjans, H., & Spener, F. (1988) *Eur. J. Biochem. 170*, 565.
Small, D. M. (1986) in *The Physical Chemistry of Lipids*, Plenum Press, New York.
Spencer, R. D., & Weber, G. (1970) *J. Chem. Phys. 52*, 1654.
Storch, J., Bass, N. M., & Kleinfeld, A. M. (1989) *J. Biol. Chem. 264*, 8708.
Sweetser, D. A., Birkenmeier, E. H., Klisak, I. J., Zollman, S., Sparkes, R. S., Mohandas, T., Lusis, A. J., & Gordon, J. I. (1987a) *J. Biol. Chem. 262*, 16060.
Sweetser, D. A., Heuckeroth, R. O., & Gordon, J. I. (1987b) *Annu. Rev. Nutr. 7*, 337.
Thumser, A. E., & Wilton, D. C. (1994) *Biochem. J. 300*, 827.
Trotter, P. J., & Storch, J. (1989) *Biochim. Biophys. Acta 982*, 131.
Wilton, D. C. (1989) *Biochem. J. 261*, 273.
Wolber, P. K., & Hudson, B. S. (1981) *Biochemistry 20*, 2800.

BI961392I